# Regional and Stratigraphic Variation in Bottomwater Anoxia in Offshore Core Shales of Upper Pennsylvanian Cyclothems from the Eastern Midcontinent Shelf (Kansas), U.S.A.

by

David L. Hoffman, Thomas J. Algeo, J. Barry Maynard,
Michael M. Joachimski, James C. Hower, and Jacek Jaminski

with 14 figures and 1 table

**Abstract**: Bottomwater oxygen levels, an important control on the preservation and quality of sedimentary organic matter, can be reconstructed on the basis of faunal, ichnofabric, and geochemical data. Patterns of variation in dissolved $O_2$ levels and its relation to organic matter cycling were investigated in Upper Pennsylvanian offshore black shales of the Eastern Midcontinent Shelf using a hierarchical sampling strategy combined with a microstratigraphic analytical approach. Sampling was undertaken of (1) multiple stratigraphic horizons (the Hushpuckney, Stark, and Muncie Creek shales), (2) multiple locales within two horizons (Hushpuckney and Stark shales), representing 150- to 200-km-long proximality gradients, and (3) dm-thick compositional cycles within each study unit. The microstratigraphic investigative procedure entailed X-radiographic, petrographic, Leco, XRF, and DOP analyses of sample zones at a sub-cm scale of resolution. Hierarchical sampling permitted reconstruction of patterns of environmental variation at both a detailed and a broad scale, allowing fuller analysis of the controls on organic matter accumulation.

An absence of bioturbation suggests uniformly anoxic conditions (0-0.2 ml $O_2$ $l^{-1}$ $H_2O$) during deposition of the Hushpuckney and Stark shales, and limited burrowing suggests anoxia grading into dysoxia (0.2-0.5 ml $O_2$ $l^{-1}$ $H_2O$) within the Muncie Creek Shale. Correlation of ichnofabric and trace-element data assisted in defining the lower and upper boundaries of the anoxic zone, which correspond to concentration ratios of 25 and 6 for Mo/TC • $10^4$, 12 and 1.5 for $U_{exc}$/TC • $10^4$, 0.9 and 0.6 for V/(V+Ni), and 5 and 1.0 for V/Cr, respectively. Regional and stratigraphic variation in redox-sensitive trace elements allowed mapping of spatio-temporal fluctuations in dissolved $O_2$ levels, revealing (1) northward intensification of bottomwater anoxia within the Hushpuckney and Stark shale environments, and (2) systematic differences between study formations, with the most and least strongly $O_2$-depleted conditions associated with the Stark and Muncie Creek shales, respectively. Organic matter in the study units may include components of both terrestrial higher plant and marine algal origin, and increases in the relative abundance of the latter are correlated with decreasing bottomwater $O_2$ levels. Sulfate reduction was most vigorous in the Stark Shale, probably owing to larger quantities of labile organic matter as a result of a near-total lack of aerobic decay at the sediment-water interface, and authigenic phosphate formation was greatest in the Hushpuckney Shale, probably as a consequence of large fluctuations in bottomwater $O_2$ levels that favored retention of P within the sediments via redox cycling of Fe.

## Introduction

Knowledge of dissolved oxygen levels in aqueous environments is important for understanding controls on the preservation and quality of sedimentary organic matter. In geologic facies in which direct measurements of dissolved oxygen are not possible, oxygen levels are estimated on the basis of faunal composition (e.g., Wignall and Myers, 1988), ichnofabric criteria (e.g., Savrda and Bottjer, 1991), or geochemical indices (e.g., Jones and Manning, 1994). Studies of the two former parameters

J. Schieber, W. Zimmerle & P. Sethi (eds.), Shales and Mudstones I

have led to recognition of oxygen-related biofacies, in which faunas characteristic of different $O_2$ concentration ranges are termed aerobic, upper dysaerobic, lower dysaerobic, and anaerobic (Rhoads et al., 1991; Wignall, 1994). The corresponding environmental terms are oxic (>2.0 ml $O_2$ $l^{-1}$ $H_2O$), weakly dysoxic (0.5-2.0 ml $l^{-1}$), strongly dysoxic (0.2-0.5 ml $l^{-1}$), and anoxic (<0.2 ml $l^{-1}$), although the oxygen levels associated with each zone are only approximately known (Wignall, 1994; n.b., for economy, the weakly and strongly dysoxic zones will henceforth be termed "suboxic" and "dysoxic," respectively). Dissolved oxygen concentrations may be expressed as a function of depletion from a baseline representing fully oxic conditions, in which case the term degree-of-anoxia (DOA) is used (Van Cappellen and Ingall, 1994).

The relative utility of different DOA indicators varies with oxygen level. Faunal data are most useful in the oxic-suboxic range, because skeletonized benthos are generally excluded at lower oxygen concentrations (Rhoads et al., 1991; Wignall, 1994). Ichnofabric data are most useful in the suboxic-dysoxic range, at which $O_2$ levels are sufficiently high to support a soft-bodied benthos but sufficiently low to prevent complete sediment homogenization (Savrda and Bottjer, 1991; Savrda et al., 1991). Geochemical data are probably most useful under anoxic conditions, in which sediments are laminated and lack paleoecological features, and in which minor variations in $O_2$ levels influence cycling of redox-sensitive compounds (Lewan and Maynard, 1982; Coveney et al., 1991; Hatch and Leventhal, 1992; Jones and Manning, 1994). Because the presence of even minute quantities of dissolved oxygen may have a profound effect on the quality of sedimentary organic matter (Canfield, 1994; Tyson, 1995), it is important to determine whether geochemical indices can discriminate effectively among different $O_2$ concentrations within the anoxic range.

In order to investigate geochemical DOA indices, we undertook a detailed study of offshore (core) black shales from Upper Pennsylvanian cyclothems of midcontinent North America. A critical but commonly insufficiently considered facet of such studies is sampling strategy. Analysis of environmental redox trends in the present study units was facilitated by our sampling strategy: (1) three different stratigraphic horizons were chosen in order to compare environmental parameters through time, (2) for two study horizons, multiple locales were chosen along a depositional proximality trend in order to investigate lateral environmental gradients, and (3) in each study unit, whole-core X-radiography was used to identify gross patterns of compositional variation, and a hierarchical sampling procedure was used to characterize such variation both at a fine (sub-cm) scale and over the full (0.4-0.6-m) thickness of each unit. This strategy met the dual objectives of (1) providing a broad spatio-temporal framework for analysis of DOA and controls on organic matter preservation, while (2) allowing investigation of lamina-scale compositional variation, which is invaluable in reconstructing "instantaneous" conditions and short-term changes in the depositional and early diagenetic environments (cf. Jaminski et al., this volume).

## Paleogeographic and Paleoclimatic Setting

Upper Pennsylvanian strata of midcontinent North America are exposed in a 500-km-long belt extending from Oklahoma in the south to Iowa and Nebraska in the north. The five cores of the present study are located in eastern Kansas, within the central part of this outcrop belt, and span a distance of ca. 200 km (Fig. 1). The study cores provide a paleoenvironmental transect across the Eastern Midcontinental Shelf with more proximal settings to the north and more distal settings to the south (Fig. 2). In southeastern Kansas, the southern margin of the shelf was approximately coincident with the east-west-trending boundary between the phylloid algal mound and terrigenous detrital facies belts of Heckel (1977; Fig. 1), but to the east it may have trended northeastward into central Missouri. From a paleotectonic perspective, the Eastern Midcontinent Shelf was separated

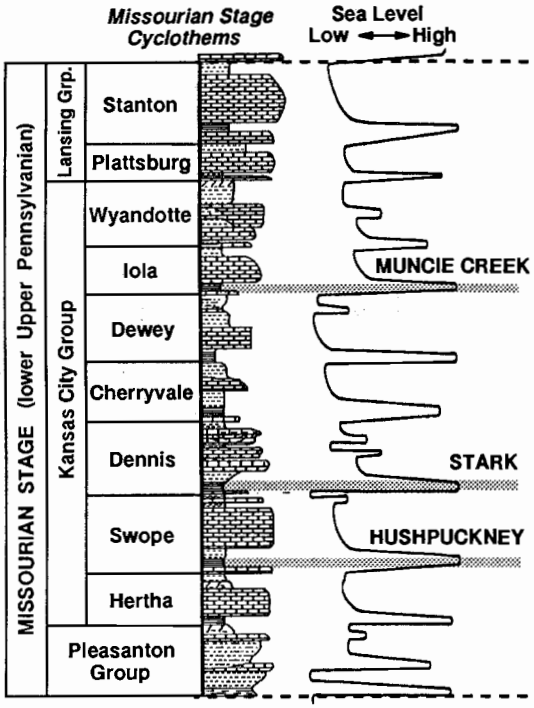


Fig. 3: Missourian Stage stratigraphy of eastern Kansas. The three stratigraphic horizons examined in this study are the Hushpuckney, Stark, and Muncie Creek shales, which represent the offshore black shale members of the Swope, Dennis, and Iola cyclothems, respectively. Sea-level curve redrawn and vertically rescaled from Boardman and Heckel (1989).

offshore shales subsequently will be referred to as "formations"). All three study formations have been designated "Heebner-type" shales, i.e., laminated, phosphatic shales containing a high proportion of organic matter of marine origin (Schultz and Coveney, 1992). In the study cores, offshore shales are thin, dark gray to black, and sparsely fossiliferous. Their contacts with subjacent transgressive limestones are sharply defined, although burrows in the underlying carbonates are commonly filled with dark shaly material and the lowermost few centimeters of some core shales contain a carbonate fossil lag. The laminated, organic-rich facies of the core shales averages 50(±10) cm in thickness and consists of alternating bands of dark gray (Munsell 10 YR 6/1-5/1) to black shale (Munsell 10 YR 3/1-2/1). These couplets, which range from about 5 to 15 cm in thickness, are weakly visible on the surface of study cores but are strongly enhanced in X-radiographs. The lighter bands in X-radiograph negatives (darker in prints such as Figure 5) contain lower concentrations of organic matter (<20 wt% C) and, in some units, larger quantities of finely disseminated Fe-sulfides (>3 wt% S) and laminar or nodular phosphatic layers of authigenic origin. In contrast, the darker bands (lighter in prints) contain higher concentrations of organic matter (to 40 wt% C) and lesser quantities of Fe-sulfides and phosphates (Fig. 5). The laminated, organic-rich facies grades upward into a progressively more intensely bioturbated gray-shale facies that contains *Chondrites*, *Zoophycos*, *Teichichnus*, and *Thalassinoides*(?) burrows to 1.0 cm in diameter (M. Droser, pers. comm., 1996). The gray-shale facies grades into a shaley carbonate facies, together comprising a ca. 0.3-1.0-m-thick transition zone between the core shale and overlying regressive limestone. Fineness of grain size,

presence of authigenic phosphate, absence of biota other than rare pelagic or epipelagic marine organisms, and $^{34}S$-depleted Fe-sulfides indicate slow accumulation of core shales in a distal offshore setting (i.e., under sediment-starved conditions) within a stratified anoxic marine basin (Heckel, 1977, 1991; Coveney and Shaffer, 1988).

## Methods

**Choice of Study Units:** The present study comprises a total of eight study units, representing three different formations (i.e., the Hushpuckney, Stark, and Muncie Creek shales) in five cores (Fig. 4). The Hushpuckney and Stark shales were examined in three and four of the five study cores, respectively, representing north-south transects of ca. 150 km (Hushpuckney) and ca. 200 km (Stark) along the Eastern Midcontinent Shelf (Fig. 1). In the description of geographic trends, the Edmonds core will be referred to as a northern locale, the Womelsdorf, Ermal, and Mitchellson cores as midshelf locales, and the Heilman core as a southern locale. The Muncie Creek Shale was examined in a single core in order to compare compositional parameters between offshore black shales of the lower (Hushpuckney, Stark) and upper (Muncie Creek) Missourian Stage. As an added control, all three formations were studied at the same locale (i.e., the Edmonds core; Fig. 4). The exact choice of study units was dictated by the availability and condition of cores at the Kansas Geological Survey.

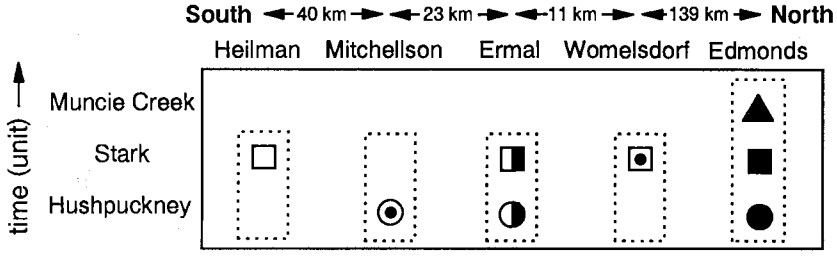


Fig. 4: Time-space distribution of the eight study units (symbols). The five cores used in this study are shown on the ordinate and the three stratigraphic horizons of interest on the abscissa. The dotted boxes enclose all offshore shales present in a given study core, some of which were not examined. The same symbols are used for identification of study units in subsequent figures.

**X-radiography:** Because fine (sub-cm) analysis of compositional variation is prohibitively labor-intensive for long stratigraphic intervals, most geochemical studies of laminated black shales have resorted to either (1) low sample density, which may overlook patterns of geochemical variation at length scales shorter than mean sample spacing (e.g., Coveney, 1985; Coveney et al., 1987; Schultz and Coveney, 1992), or (2) restriction of analysis to short stratigraphic intervals, which limits the overall spatio-temporal scope of investigation (e.g., Wenger and Baker, 1986; Desborough et al., 1991; Hatch and Leventhal, 1992). Jaminski and others (Shales and Mudstones I) overcame this problem by combining whole-core X-radiography with a hierarchical subsampling strategy for petrographic and geochemical characterization of the study units, and a similar approach was utilized in the present study. The X-radiographic procedures were identical to those of Jaminski and others (Shales and

Mudstones I) except that gray-scale density (GSD) values were measured in three parallel line transects (i.e., along the center of the long axis of each core segment and 5 mm to either side of the center), which were averaged to produce a single composite GSD record (Fig. 5). Pronounced lateral compositional variability at a centimeter scale made averaging of multiple parallel GSD transects desirable for Midcontinent Pennsylvanian black shales.

**Sampling Procedure:** Within each of the eight study units, a single 8- to 15-cm-thick interval was chosen for detailed petrographic and geochemical analysis (Fig. 5). Approximately correlative horizons were sampled to facilitate inter-core comparisons, and the lower to middle portion of the black-shale facies was favored for this purpose owing to (1) presence of well-defined dm-scale compositional cycles, and (2) ease of correlation between cores (n.b., compositional patterns within a given formation are most similar in the lowermost 30 cm of each study unit). Each core interval chosen for detailed analysis was located so as to include at least one complete dm-scale compositional cycle. Each core interval was subdivided into 8-13 sample zones of subequal thickness (0.6-2.0 cm; mean 1.0 cm), yielding a total of 85 samples from the eight study units. Contacts between sample zones were picked on the basis of core X-radiographs so that the boundaries coincided with natural compositional breaks (Fig. 5). Each interval was split longitudinally (i.e., parallel to the core axis) into two halves, one of which was epoxied for petrographic analysis and the other of which was ground for geochemical analysis. Powdered samples were stored in nitrogen-filled vials and refrigerated to prevent oxidation of organic carbon and sulfides prior to analysis. The same 0.6-2.0-cm-thick sample zones were used for all procedures, including petrographic, C-S, major- and trace-element, and DOP analyses.

**Carbon-Sulfur Elemental Analysis:** Carbon and sulfur elemental concentrations were measured on a whole-rock basis, yielding total carbon (TC) and total sulfur (TS) values in weight percent, using a LECO CS-244 analyzer at the Kentucky Geological Survey. A laboratory standard was run before and after each set of fifteen samples to monitor instrument drift. Analytical precision ($2s$) was ±2.0 % for TC and ±7.6 % for TS of measured concentrations based on 15 replicate analyses. A total of 106 samples were analyzed, i.e., the 85 samples from the eight core intervals chosen for detailed study (see sampling procedure above) plus another 21 samples from the base and top of the Stark Shale at several locales; the latter set was intended to document stratigraphic variation in TC and TS content within this formation. A representative subset of samples from all study formations and locales ($n$ = 17) was analysed for inorganic C content using a carbonate bomb; because these samples yielded such low mean inorganic C values (1.2±0.9 % of total carbon), it was deemed unnecessary to run this procedure for the full sample set. A small number of samples will be analyzed for DOP (degree-of-pyritization) using the chromium reduction technique of Canfield et al. (1986), but this analytical step has not been completed yet.

**Petrographic Analysis:** Petrographic components were examined in polished slabs under both reflected white and violet-UV fluorescent light, and organic macerals were classified using standard terminology (Hutton, 1987; Tyson, 1995). For each sample zone, a minimum of 300 observations were collected such that all linear traverses perpendicular to bedding were completed. Point-counts were undertaken only on sample zones consisting of fine-grained organic and detrital matter ($n$ = 56) and not on those representing phosphate nodules. Within the organic-detrital intervals, phosphate may have been present as a cement but was not recognizable as such; hence, phosphate is not included in the point-count tallies.

**Organic Carbon Isotopic Analysis:** About half of the samples were analyzed for bulk organic carbon $\delta^{13}C$. Samples were with hot concentrated HCl to remove carbonates and then washed with deionized water to neutrality. Samples were combusted with CuO at 850°C in quartz tubes, and the evolved $CO_2$ was purified by cryogenic distillation. Isotopic analyses were performed at the University of Erlangen-Nürnberg using a Finnegan MAT 252 mass spectrometer. Reproducibility was checked by repeated measurements of graphite standard USGS 24 and is better than ±0.1 ‰.

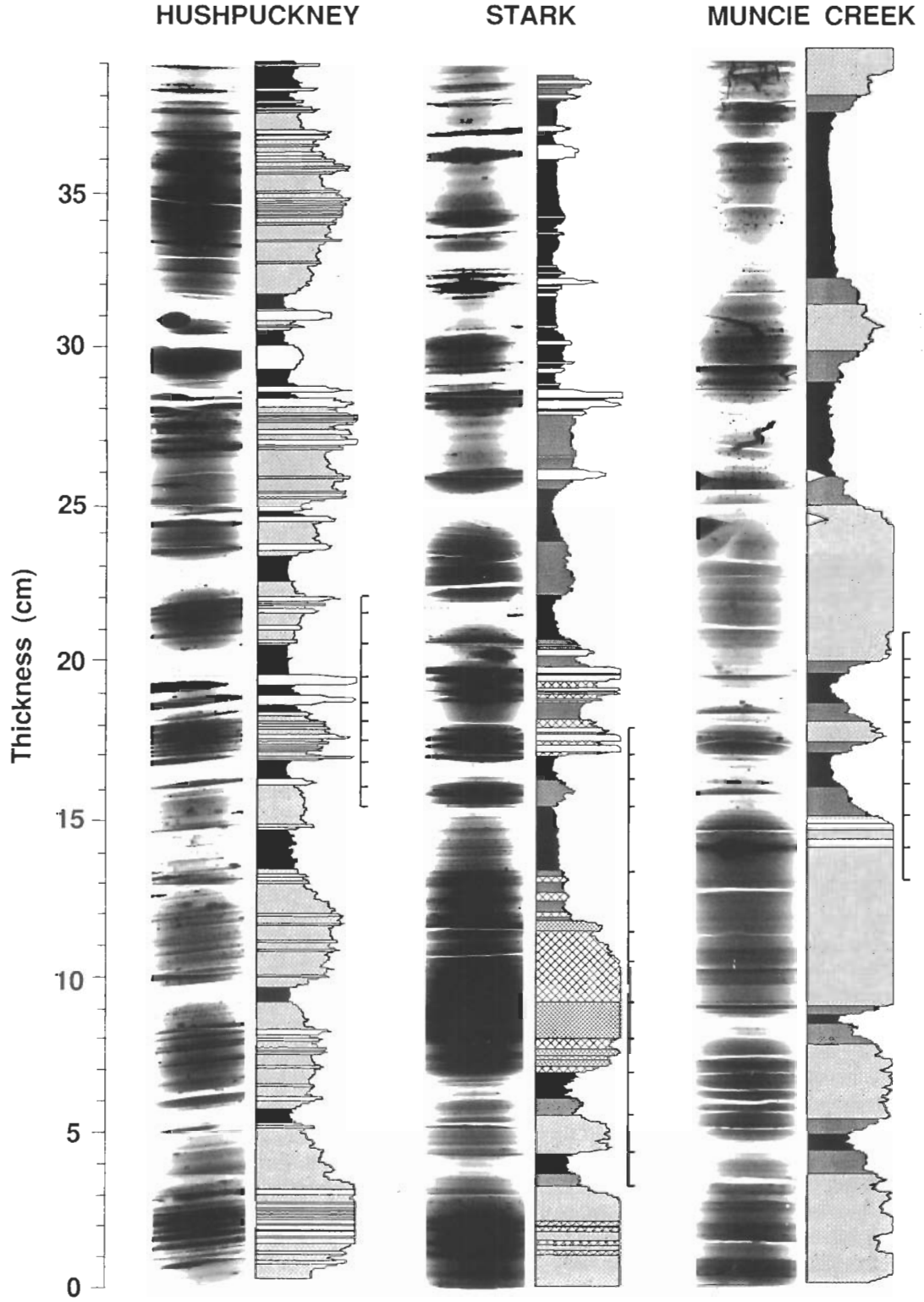
HUSHPUCKNEY
STARK
MUNCIE CREEK
Thickness (cm)
35
30
25
20
15
10
5
0

**Major- and Trace-Element Analysis:** About 3-4 g from each sample zone were pressed into a pellet and analyzed for whole-rock elemental concentrations using a wavelength-dispersive Rigaku 3040 XRF spectrometer at the University of Cincinnati. See Jaminski and others (this volume) for procedural details, analytical precision, and detection limits.

## Results

**X-radiography:** Whole-core X-radiography was used to visually identify patterns of compositional variation within the study units and to quantify this variation based on GSD-elemental correlations (e.g., Fig. 5). Contrast in X-radiographs is a function of the abundance and distribution of components that differ in density from the clay matrix of the shale (2.6-2.7 g $cm^{-3}$), i.e., organic carbon (1.0-1.2 g $cm^{-3}$), phosphate (3.1-3.2 g $cm^{-3}$), and pyrite (5.1-5.2 g $cm^{-3}$; cf. Algeo et al., 1994). GSD variation in the study units is controlled mainly by organic carbon (as proxied by TC), which accounts for 27 % ($p(\alpha) < .10$), 63 % ($p(\alpha) < .01$), and 92 % ($p(\alpha) < .01$) of total GSD variance in the Hushpuckney, Stark, and Muncie Creek shales, respectively. GSD values are influenced by phosphorus ($P_2O_5$) in the Hushpuckney Shale (26 % of total GSD variance; $p(\alpha) < .10$), which contains a greater abundance of phosphate nodules than the Stark and Muncie Creek shales. Fe-sulfides vary in concentration to a limited degree in the study units and, with the exception of the Stark Shale in the Heilman core, exert only a weak influence on GSD values.

X–radiographs of the study cores permitted detailed observations regarding compositional layering, ichnofabrics, and the distribution of authigenic precipitates. Compositional layering is present

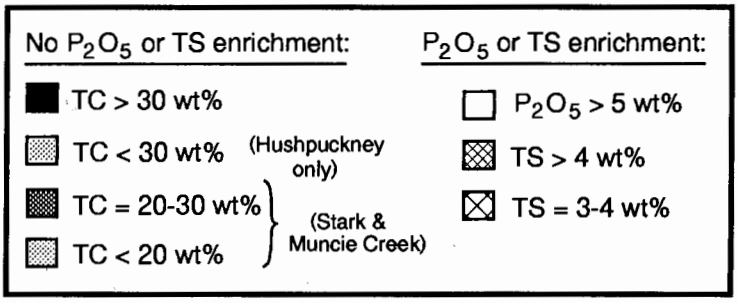


Fig. 5: (A) X-radiographs of the Hushpuckney, Stark, and Muncie Creek shales in the Edmonds core (left-hand column of each pair of columns). Scale to left of figure gives thickness above the base of the laminated black-shale facies; ca. 80 % of the total thickness of the black-shale facies is shown for the Hushpuckney and Stark shales and 100 % for the Muncie Creek Shale. Note burrows in the Muncie Creek Shale above 25 cm. These images are positive X-radiograph prints, in which denser features appear darker. In the right-hand columns, column relief gives gray-scale density (GSD) as measured along the center of the long axis of each X-radiograph image to the left, and the shaded fill patterns represent the (measured or inferred) geochemical composition of each layer in the core. Compositions were analytically determined within the intervals marked by heavy graduated lines (ticks denote boundaries of sample zones) and were estimated on the basis of GSD-TC-TS correlations outside of the sampled intervals. Phosphate-rich intervals were identified through visual inspection of cores and X-radiographs; sampled intervals containing macroscopic phosphate nodules yielded 5-8 wt% $P_2O_5$ and those lacking nodules <0.5 wt% $P_2O_5$. (B) Legend for shaded fill patterns used in the geochemical composition columns in part A of figure. Total carbon (TC) values are given for core intervals without phosphate or sulfide enrichment; intervals containing >5 wt% $P_2O_5$ (i.e., phosphate nodules) or >3 wt% TS (i.e., sulfide-rich layers) are identified separately.

throughout the laminated black-shale facies of all study units at several scales: (1) as faint, horizontal, sub-mm-thick laminae, and (2) as dm-scale bands consisting of alternating dark (high-TC) and light (low-TC) layers (Fig. 5). The dm-scale compositional bands are readily correlatable within a given formation across the 200-km-long study area. Bioturbation of the laminated black-shale facies of the study units is limited: the Hushpuckney and Stark shales exhibit no evidence of benthic activity, but the Muncie Creek Shale contains isolated, 3- to 4-mm-diam. *Chrondrites* burrows in its upper half (>25 cm above base of section; Fig. 5). Authigenic sulfides and phosphates appear as dark (high-density) features in core X-radiographs. The distribution of sulfides is difficult to ascertain owing to fine dissemination through the shale matrix, but phosphate is easily recognized by its distinctive morphology, e.g., smooth ovoid nodules, small granules, and wispy laminae. Authigenic phosphate is found mainly within or at the contacts of high-TC layers and, hence, appears to exhibit an association with organic carbon. Although present in all study units, the abundance of authigenic phosphate varies between formations, being greatest in the Hushpuckney Shale and least in the Muncie Creek Shale (Fig. 5).

**Elemental Associations:** Elemental associations in the study units were investigated via R-mode cluster analysis of matrices of Pearson correlation coefficients ($r$) for elemental concentration pairs. The resulting dendrograms yielded elemental affinity groups corresponding to each of the main components of the study units identified by X-radiography. Cluster analysis of samples from all study units ($n$ = 85) revealed organic, phosphatic, and detrital affinity groups (Fig. 6), while dendrograms for individual study units (not shown; $n$ = 8-13 per unit) commonly contained a sulfidic affinity group that variably included Fe, Mn, V, Mo, Cr, and Zn. Results of the cluster analyses for individual study units are summarized in Table 1, in which elements are listed by dominant affinity (i.e., the most common association among the eight study units), while secondary affinities (i.e., those observed in at least one study unit) are given in parentheses. Although many elements exhibited the same association in all study units, some elements exhibited variable affinities, especially those for which the dominant association was organic (Table 1). General controls on trace-element associations were considered by Jaminski and others (this volume), so discussion below will focus on elemental relations indicative of redox conditions and organic cycling processes.

Cluster analyses included one elemental parameter that was calculated rather than measured, "excess" uranium ($U_{exc}$). Although the dominant affinity of U in the study units is phosphatic (Fig. 6; Table 1), cross-plots of total uranium ($U_{tot}$) versus phosphorus ($P_2O_5$) indicate the presence of two U components (Fig. 7). Within each study unit, $U_{tot}$ and $P_2O_5$ exhibit a positive Y-intercept and moderate to strong positive covariance (cf. Desborough et al., 1991). This pattern suggests that (1) positive covariation of $U_{tot}$ and $P_2O_5$ above a unit-specific baseline value (Y-intercept) is due to a uranium component associated with phosphorus, probably U adsorbed onto phosphate nodule surfaces (Jarvis et al., 1994), (2) differences in the slope of the $U_{tot}$-$P_2O_5$ relation may be due to differences in the specific surface area or growth rates of phosphate nodules in different formations, and (3) the Y-intercept represents the average content of "excess" (i.e., non-phosphatic) uranium ($U_{exc}$) in a given study unit. For individual samples, excess uranium was calculated as:

$$U_{exc}(i,j) = U_{tot}(i,j) - m(j) \bullet P_2O_5(i,j) \quad (1)$$

where $U_{tot}(i,j)$ and $P_2O_5(i,j)$ are the measured total uranium and phosphorus concentrations of sample $i$ in study unit $j$, and m(j) is the slope of the $U_{tot}$-$P_2O_5$ relation for study unit $j$ (Fig. 7). Excess uranium correlates positively with TC and clusters with the organic affinity group (Fig. 6), suggesting that it is present as an adsorbed phase on organic matter. As such, it is equivalent to the "authigenic uranium" of Wignall and Myers (1988), but the latter term would be inappropriate here given the authigenic origin of both the phosphatic and non-phosphatic uranium fractions.

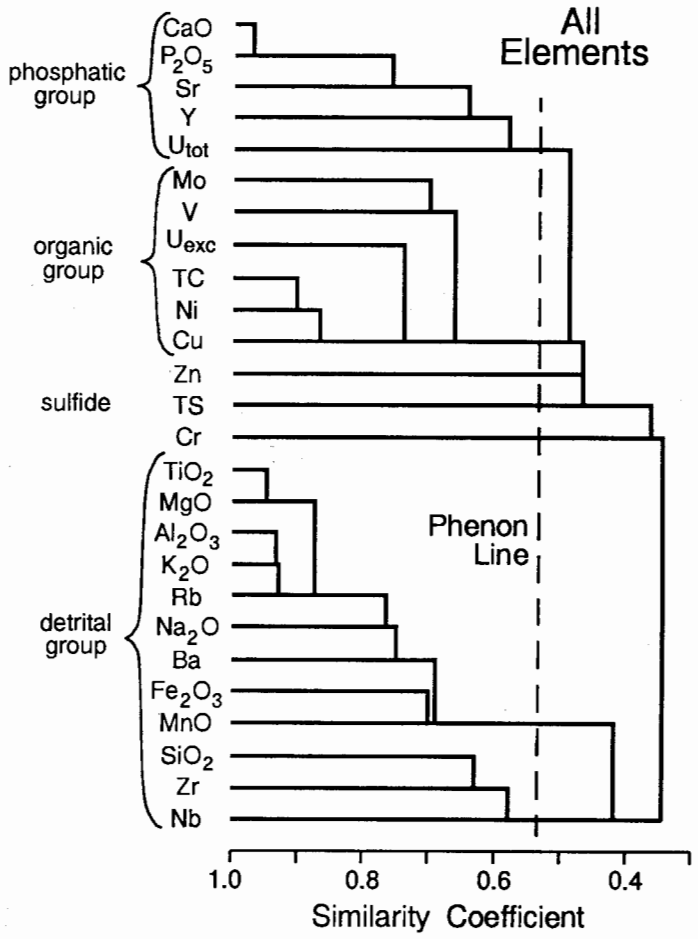


Fig. 6: Dendrogram of major- and trace-element relations based on R-mode cluster analysis; the distance metric was the Pearson correlation coefficient ($r$) and the linkage protocol was the weighted pair-group centroid method. Phenon lines were chosen to (1) coincide with similarity coefficient ranges containing few linkages and (2) yield a small number of interpretable elemental clusters. The results shown are based on all samples from the study units ($n$ = 85); similar results were obtained for individual offshore shales. See text for discussion of elemental affinity groups.

The two dominant maceral types, vitrinite and inertinite, vary in relative abundance as a function of geographic location within individual study formations. The geographic influence on I/V ratios is most readily observed for the Stark Shale, in which northern locales yield low I/V ratios (<0.4), midshelf locales intermediate I/V ratios (0.4-0.7), and southern locales high I/V ratios (0.9-1.1; Fig. 8A). A weak geographic trend also may exist for organic carbon $\delta^{13}C$ in the Stark Shale, in which mean $\delta^{13}C$ values are more depleted at northern locales (-28.1±0.3) than at midshelf (-27.7±0.3) or southern locales (-27.7±0.6; Fig. 8B); recognition of geographic trends in $\delta^{13}C_{org}$ in the Hushpuckney and Muncie Creek shales is precluded by an insufficient number of analyzed locales. Differences in I/V ratios are also apparent between study formations at a single locale (i.e., the Edmonds core): at a given volumetric fraction of organic matter, the Stark Shale exhibits comparatively low I/V ratios, the Hushpuckney Shale intermediate values, and the Muncie Creek Shale high values (Fig. 8A). The study formations exhibit substantial differences in mean $\delta^{13}C$ values, with the Hushpuckney Shale being significantly $^{13}C$-depleted (-28.3±0.8 ‰ PDB; $n$ = 20)

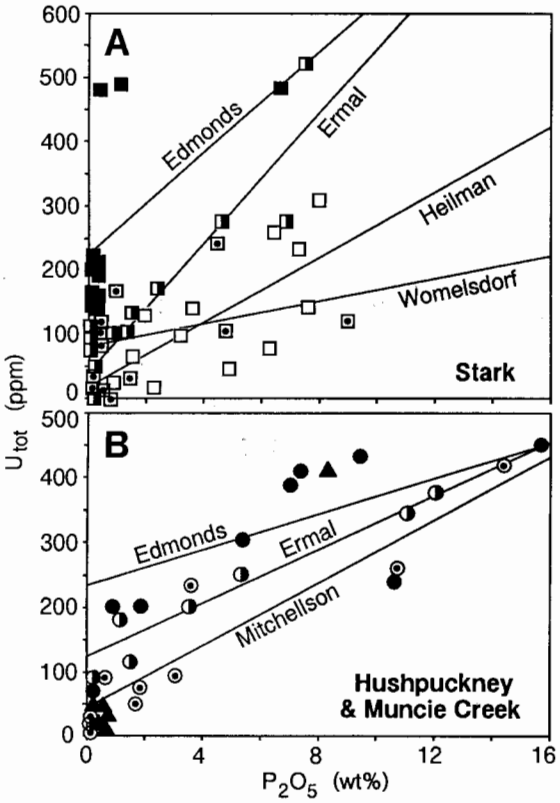


Fig. 7: Uranium-phosphorus relations in the Stark (A) and Hushpuckney and Muncie Creek shales (B); symbols as in Fig. 4. Each study unit exhibits (1) positive $U_{tot}$-$P_2O_5$ covariation, indicating presence of a U component associated with P, and (2) a positive Y-intercept, indicating presence of a non-phosphatic ("excess") U component that is probably an adsorbed phase on organic matter. Regression lines for each unit, which are based only on $P_2O_5$ values >0.5 wt%, are used in calculating excess uranium values ($U_{exc}$; eq. 1 in text).

relative to the Muncie Creek (-27.4±0.3 ‰ PDB; $n$ = 6) and Stark shales (-27.6±0.5 ‰ PDB; $n$ = 35; Fig. 8B).

**Carbon-Sulfur-Iron Systematics:** Organic matter and sulfides are two of the major components of the study units (Fig. 5; Table 1). A near-absence of inorganic carbon (i.e., carbonate C) is indicated by (1) point-counts yielding a mean $CaCO_3$ abundance of <1 vol%, and (2) carbonate bomb analyses yielding a mean inorganic C fraction of 1.2±0.9 % of total carbon ($n$ = 17). Hence, total carbon (TC), which ranges from <10 to >40 wt% in samples from the study units, is an effective proxy for total organic carbon (TOC). Organic matter in offshore shales of eastern Kansas is of relatively low maturation rank (Wenger and Baker, 1986), so thermal alteration is not a major concern. Sulfur is present mainly in Fe-sulfides such as pyrite and, to a more limited degree, in organic matter and phosphate nodules. Estimates of mean pyrite abundance based on petrographic point-counts (8±8 vol%) are probably too high but serve to verify the presence of a substantial Fe-sulfide component.

Iron is an important component of black shales owing to its sensitivity to redox changes and uptake in Fe-sulfides. In the study units, Fe is present in considerable amounts in excess of that needed for formation of stoichiometric pyrite (i.e., a 2:1 S:Fe ratio; Fig. 9), indicating the presence of a non-sulfide Fe-bearing phase. This phase is likely to be a clay mineral such as Fe-chlorite (cf. Desborough et al., 1991), from which iron is not readily liberated for Fe-sulfide formation (Canfield

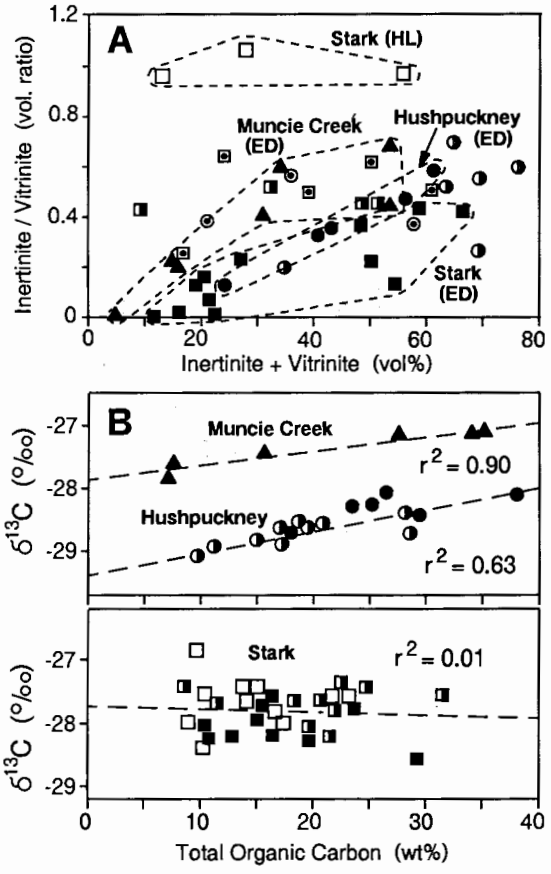


Fig. 8: Variation in organic maceral frequency ratios (A) and organic carbon C-isotopic compositions (B) as a function of total organic carbon concentration (n.b., given as volume percent in A and as weight percent in B; symbols as in Fig. 4). Note (1) positive covariation of inertinite/vitrinite ratios with TOC for all three shales at the Edmonds locale (ED; dashed fields) in A, and (2) positive covariation of organic carbon $\delta^{13}C$ values with TOC for the Hushpuckney and Muncie Creek shales in B.

et al., 1992). Nonetheless, the study units exhibit moderate to high degrees of sulfidation of iron. $DOP_{tot}$ calculations, which assume that all iron is reactive and available for Fe-sulfide formation (cf. Jaminski et al., this volume), yield high values (ca. 0.5-0.8) for the Stark and Hushpuckney shales, indicative of strong anoxia, and lower values (ca. 0.3) for the Muncie Creek Shale, implying somewhat weaker anoxia (Fig. 9). To the degree that excess Fe in the study units is present in unreactive mineral phases, true DOP values would be higher than the estimates above and imply more intense anoxia in the study units. Two study units, the Stark Shale in the Edmonds and Ermal cores, exhibit strong positive S-Fe covariation, whereas the other six study units do not (Fig. 9); such covariation is consistent with strong anoxia and a high degree of Fe-sulfidation.

TC-TS values in all three study formations fall well below the "normal" marine trend for oxic-suboxic environments (Berner and Raiswell, 1983) and exhibit large, positive regression Y-intercepts (1.0-1.8 wt% TS; Fig. 10). TC and TS concentrations are only weakly correlated in the Muncie Creek and Stark shales ($r^2$ = 0.10 and 0.15, respectively) but covary strongly in the Hushpuckney Shale ($r^2$ = 0.46). Furthermore, the four study units of the Stark Shale exhibit widely different TC-TS

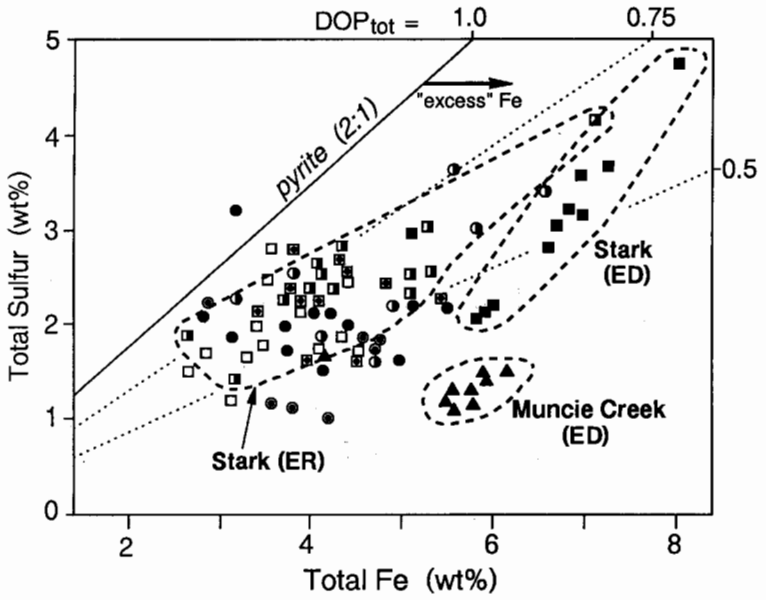


Fig. 9: Sulfur-iron relations for all samples from the study units ($n$ = 85); Fe values are given as elemental rather than oxide concentrations; symbols as in Fig. 4. A S:Fe ratio of 2:1 for stoichiometric pyrite is shown at left; note that most samples contain "excess" Fe. $DOP_{tot}$ values of 0.5, 0.75, and 1.0 are shown as diagonal lines; a $DOP_{tot}$ of 1.0 coincides with the pyrite line. Note that (1) most $DOP_{tot}$ values for the Stark and Hushpuckney shales are high (>0.5), (2) S-Fe covariation is significantly positive for the Stark Shale in the Edmonds (ED) and Ermal (ER) cores (dashed fields) but no S-Fe covariation is observed for the Hushpuckney Shale, and (3) most $DOP_{tot}$ values for the Muncie Creek Shale are low (ca. 0.3).

correlations, whereas all three study units of the Hushpuckney Shale exhibit positive correlation coefficients ($r$) of similar magnitude (+0.58 to +0.70; Fig. 10C). These observations are consistent with strong anoxia during deposition of the study units (see above) as well as with generally Fe-limited conditions for authigenic sulfide formation. However, strong positive TC-TS covariance in the Hushpuckney Shale may indicate some control of sulfate reduction rates by the type or degree of reactivity of organic matter and, hence, imply a lesser degree of Fe-limitation than in the Stark Shale, which is consistent with the existence of S-Fe covariation in the latter formation and its absence in the former formation (Fig. 9).

**Distribution of Organic Carbon, Sulfide, and Phosphate:** Most components of the study units exhibit pronounced regional trends that may be useful in inferring environmental gradients in the depositional system (see discussion below). Among the major components, organic carbon (proxied by TC) and Fe-sulfides (proxied by TS) increase to the north in a fairly uniform manner in both the Stark and Hushpuckney shales (Fig. 11A-B). In contrast, phosphate (proxied by $P_2O_5$) increases northward in the Hushpuckney Shale but southward in the Stark Shale (Fig. 11C), a pattern that is mirrored by phosphate nodule abundances in core X-radiographs. Trace elements that have a predominantly organic affinity (e.g., Mo and $U_{exc}$; Table 1) exhibit northward increases in both absolute and TC-normalized concentrations (Fig. 11D-E); the TC-normalized values are of greater significance for environmental interpretations because they reflect redox-sensitive rates of trace-element uptake by organic matter. Trace elements of mixed organic-detrital affinity (e.g., V, Ni, and Cr; Table 1) also exhibit northward increases in concentration, but the magnitude of the increase varies in proportion to the redox sensitivity of a given element (V > Ni > Cr; Fig. 11F-G). Potentially significant is that these compositional parameters exhibit different rates of lateral variation, implying

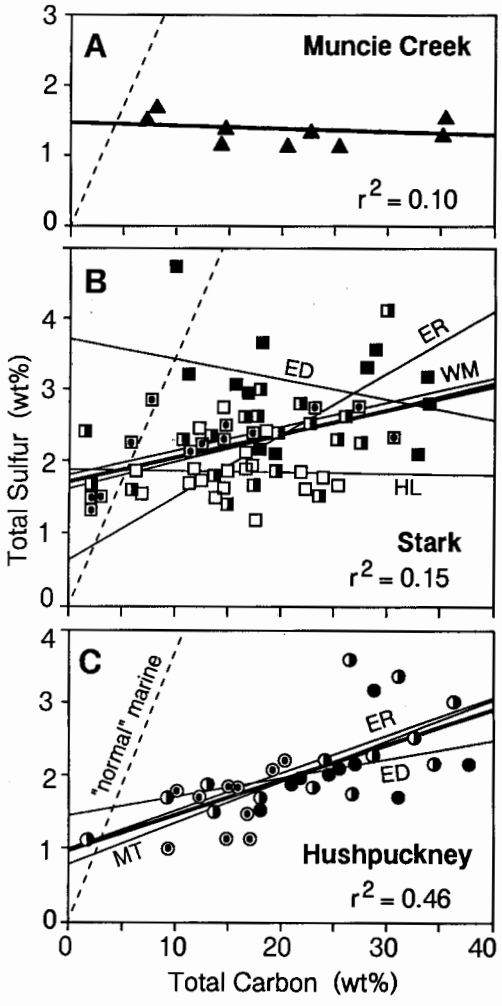


Fig. 10: Carbon-sulfur relations for the Muncie Creek (A), Stark (B), and Hushpuckney (C) shales; symbols as in Fig. 4. TC-TS regression lines are shown for samples from each study unit (thin lines) and for all samples from each offshore shale (heavy lines). Core abbreviations are Edmonds (ED), Ermal (ER), Heilman (HL), Mitchellson (MT), and Womelsdorf (WM). Coefficients of determination ($r^2$) are for all samples from a given offshore shale; $r^2$ values are significant ($p(\alpha) < .01$) for the Hushpuckney and Stark shales ($n$ = 33 and 64, respectively) and non-significant for the Muncie Creek ($n$ = 9). The C-S trend for "normal" marine shales deposited in oxic-suboxic environments (dashed line) is from Berner and Raiswell (1983).

differences either in concentration gradients or, more likely, in their sensitivity to redox changes. For example, TC and TS increase northward within the study area by a factor of 1.3-1.8 (Fig. 11A-B), but Mo/TC increases by a factor of 1.8-3.6 (Fig. 11D), $U_{exc}$/TC by a factor of 2.7-3.5 (Fig. 11E), and V/Cr by a factor of 2.2-4.1 (Fig. 11G). In addition to regional trends, the three study formations exhibit a consistent stratigraphic relationship with regard to these compositional parameters, i.e., when compared at a single locale (the Edmonds core), concentrations of TS, Mo/TC, $U_{exc}$/TC, and V/Cr are highest in the Stark Shale, intermediate in the Hushpuckney Shale, and lowest in the Muncie Creek Shale (Fig. 11; n.b., TC, $P_2O_5$, and V/(V+Ni) do not conform to this pattern).

Proxies for organic carbon, sulfide, and phosphate generally exhibit linear patterns of covariation

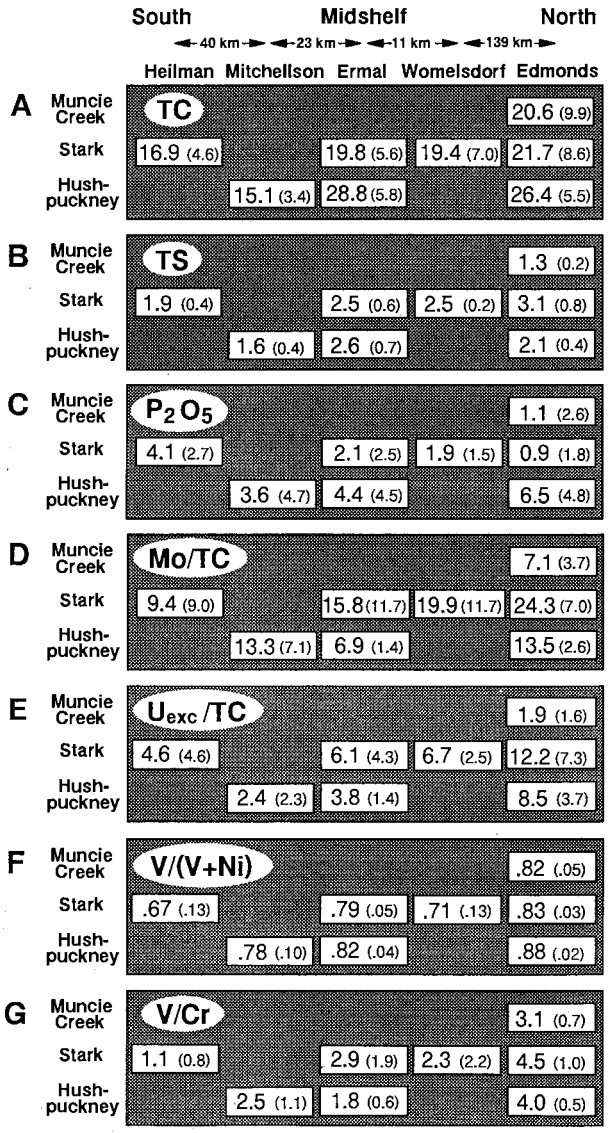


Fig. 11: Time-space variation in elemental concentrations and ratios associated with organic matter cycling and redox conditions. Shown are section-mean concentrations (with standard deviations in parentheses) for total carbon TC (A), total sulfur TS (B), phosphorus $P_2O_5$ (C), molybdenum Mo/TC (D), non-phosphatic or "excess" uranium $U_{exc}$/TC (E), vanadium:nickel ratio V/(V+Ni) (F), and vanadium:chromium ratio V/Cr (G). Concentrations of elements that are present mainly as an adsorbed phase on organic matter (e.g., Mo, $U_{exc}$, and V) must be normalized to TC; trace-element ratios (e.g., V/Cr) are implicitly normalized. Values for TC, TS, and $P_2O_5$ are in weight percent, those for Mo/TC and $U_{exc}$/TC are $10^4$ times a dimensionless weight ratio, and those for V/(V+Ni) and V/Cr are dimensionless. North is to the right and stratigraphically younger offshore shales toward the top of figure (compare format with Fig. 4). See text for discussion of significance of concentration gradients.

(Fig. 12). Because section-mean TC, TS, Mo/TC, $U_{exc}$/TC, V/(V+Ni), and V/Cr values increase to the north in both the Hushpuckney and Stark shales, correlations among these compositional parameters

are generally positive. However, some parameter pairs exhibit differences between formations that may be of environmental significance. For example, TC and TS values exhibit strong positive covariation in both the Stark and Hushpuckney shales but a slope that is about twice as steep in the former as in the latter formation (Fig. 12A). TS and $U_{exc}$/TC values exhibit a much weaker correlation in the Hushpuckney Shale than in the Stark Shale (Fig. 12B), while $P_2O_5$ and $U_{exc}$/TC values exhibit positive covariation in the Hushpuckney Shale but negative covariation in the Stark Shale (Fig. 12C). On the other hand, some compositional pairs exhibit similar covariation patterns in both formations, e.g., V/Cr and $U_{exc}$/TC values (Fig. 12D). These patterns of covariation may be useful in drawing inferences about (1) regional environmental gradients and (2) coupling between various processes associated with organic matter cycling, i.e., carbon delivery, sulfate reduction, and authigenic phosphate precipitation (see discussion below).

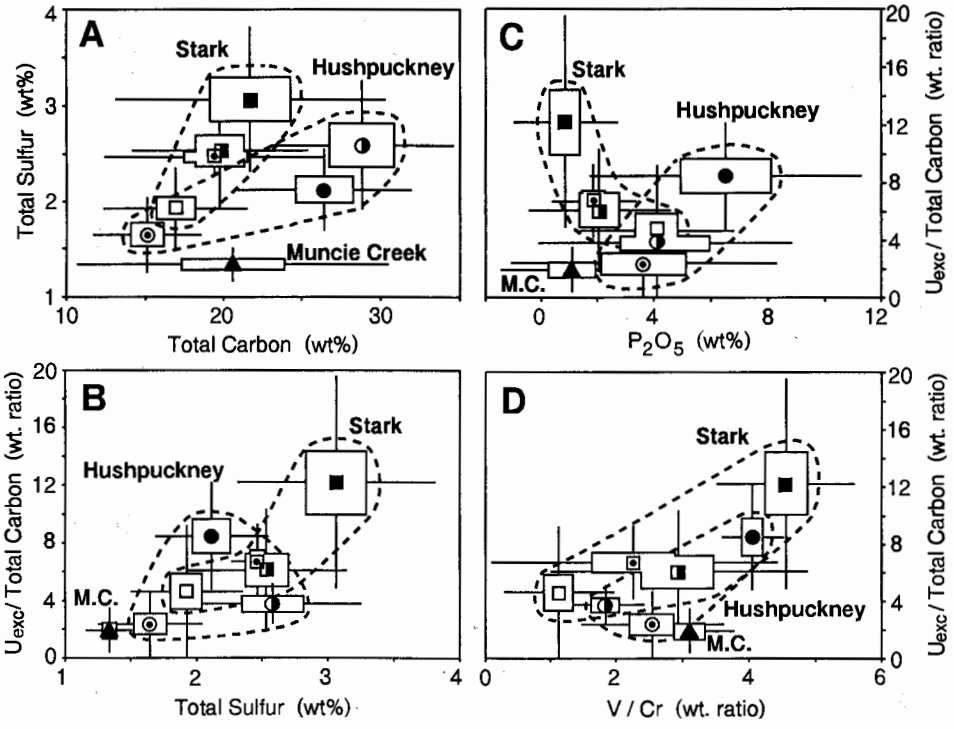


Fig. 12: Covariation patterns among elements associated with organic matter cycling and redox conditions. Section-mean values (cf. Fig. 11) are cross-plotted for TC-TS (A), TS-$U_{exc}$/TC (B), $P_2O_5$-$U_{exc}$/TC (C), and V/Cr-$U_{exc}$/TC (D). Section means are shown as symbols (see Fig. 4), ranges of the standard error of the mean $s/\sqrt{n}$ as open rectangles, and ranges of the standard deviation $s$ as crosses; section means for the Stark and Hushpuckney shales are enclosed by dashed lines to emphasize geographic trends within these formations.

## Discussion

**Degree-of-Anoxia (DOA):** Bottomwater oxygen levels during deposition of Midcontinent Pennsylvanian offshore shales can be constrained using a combination of faunal, ichnofabric, and geochemical data. Unfortunately, disagreement exists among paleoecologists with regard to the defining

characteristics of certain oxygen-related biofacies: Savrda et al.'s (1991) dysaerobic biofacies contains burrows (and, hence, a soft-bodied infauna) without a hard-shelled benthos, whereas Wignall's (1994) lower dysaerobic biofacies (ORBs 3 and 4) contains abundant hard-shelled epibionts along isolated surfaces in otherwise unburrowed sediments. This discordance is probably due to differences in temporal patterns of bottomwater oxygenation that are implicit in each model. Specifically, Savrda et al.'s model assumes gradual long-term changes in dissolved $O_2$ levels, whereas Wignall's model may reflect the effects of episodic short-term oxygenation events under otherwise anoxic conditions (to which the term "poikiloxia" may be applied). In the study units, no hard-shelled benthos and only minor burrowing was observed in the laminated black-shale facies (Fig. 5), and bioturbation preceded the appearance of a hard-shelled benthos in the overlying gray-shale facies (n.b., faunal and ichnofabric data for the latter facies will be presented elsewhere). These observations suggest that Savrda et al.'s (1991) model may be more applicable to the study units. Thus, paleoecological criteria indicate persistent anoxia (<0.2 ml $O_2$ $l^{-1}$ $H_2O$) during deposition of the black-shale facies in the Hushpuckney and Stark shales, and anoxia yielding to intermittent or permanent dysoxia (0.2-0.5 ml $O_2$ $l^{-1}$ $H_2O$) during deposition of the upper part of the black-shale facies in the Muncie Creek Shale.

Given the strongly oxygen-depleted conditions that prevailed within the study units, geochemical data may have the greatest potential for diagnosis of fluctuations in bottomwater $O_2$ levels. Concentrations or ratios of redox-sensitive trace-elements are used for this purpose (e.g., Lewan and Maynard, 1982; Coveney et al., 1991; Hatch and Leventhal, 1992). For example, sediments deposited under low-oxygen conditions are commonly enriched in Mo, U, V, Ni, and Cr because the reduced ionic species of these elements are either readily adsorbed onto organic matter or form insoluble chemical precipitates (Pratt and Davis, 1992; Calvert and Pedersen, 1993). However, trace-element concentrations in the sediment also may vary as a function of availability of preferred substrates for uptake (i.e., type of sedimentary organic matter) or as a result of buildup of trace-element concentrations in the water column via organic matter remineralization, and, hence, it is necessary to consider relations between trace elements and major components such as organic carbon, Fe-sulfide, and authigenic phosphate. Furthermore, because these components are coupled via redox-sensitive processes associated with organic matter cycling, e.g., sulfate reduction and authigenic phosphate precipitation, spatio-temporal trends in major sediment components also may provide information regarding environmental conditions. Hence, in the following discussion we will consider relations among major components and redox-sensitive trace elements in evaluating bottomwater $O_2$ levels.

**Regional Trends in DOA:** In both the Hushpuckney and Stark shales, lateral geochemical trends imply decreasing bottomwater oxygen levels to the north (Fig. 13). The strongest evidence in support of this interpretation is a pattern of northward increases by factors of two to four in the TC-normalized concentrations of redox-sensitive trace elements, e.g., Mo/TC, $U_{exc}$/TC, V/(V+Ni), and V/Cr (Fig. 11D-G). Other geochemical parameters exhibit trends that are consistent with this inference but that would be insufficient evidence thereof without the trace-element data cited above. Among the major components, both TC and TS increase northward (Fig. 11A-B). The significance of the TC trend is uncertain in the absence of information regarding productivity versus preservation controls on organic matter accumulation, although a northward increase in TC is potentially consistent with enhanced preservation of organic matter under more strongly anoxic conditions. Northward increases in TS are larger than those in TC (Fig. 11A-B), implying more intense sulfate reduction rates per unit organic carbon, which is also consistent with stronger anoxia to the north. Strong positive covariation of TS with $U_{exc}$/TC (Fig. 12B), Mo/TC, V/(V+Ni), and V/Cr (not shown) suggests a link between rates of sulfate reduction and adsorption of redox-sensitive trace elements, e.g., via stronger anoxia and/or preferential uptake of U on bacterially-degraded organic matter. In the Stark Shale, several other geochemical parameters may support northward intensification of bottomwater anoxia: (1) stronger covariation of TS and Fe to the north (i.e., Edmonds and Ermal cores; Fig. 9),

suggesting stronger Fe-limitation of sulfide formation, and (2) steeper $U_{tot}$-$P_2O_5$ correlations to the north (i.e., Edmonds and Ermal cores; Fig. 7), suggesting greater uptake of U per unit P during phosphate nodule growth. Taken together, these geochemical trends document a general increase in the intensity of bottomwater anoxia to the north (Fig. 13), which is consistent with depositional models invoking a strong proximal halocline and a weaker distal thermocline across the Eastern Midcontinent Shelf (Heckel, 1991; Hatch and Leventhal, 1992).

**Stratigraphic Trends in DOA:** Geochemical parameters suggest differences in dissolved $O_2$ levels between the study formations at the locale at which all three horizons were analyzed (i.e., the Edmonds core; Fig. 13). At this locale, section-mean Mo/TC, $U_{exc}$/TC, and V/Cr values are highest in the Stark Shale, intermediate in the Hushpuckney Shale, and lowest in the Muncie Creek Shale (Fig. 11D-E,G); the only inconsistent trace-element parameter is V/(V+Ni), which exhibits higher values in the Hushpuckney Shale than in the Stark Shale (Fig. 11F). This sequence of relative DOA values is in accord with physical evidence from the study cores (Fig. 5): (1) the Stark Shale is laminated throughout and contains only scattered phosphate nodules, consistent with poor retention of organic P under uniformly anoxic conditions, (2) the Hushpuckney Shale is laminated but contains abundant phosphate nodules, consistent with enhanced retention of organic P at low but fluctuating $O_2$ levels, and (3) the Muncie Creek Shale is partly bioturbated and contains comparatively little sulfide and phosphate, consistent with lower rates of anaerobic bacterial activity under dysoxic conditions (e.g., as a consequence of greater aerobic bacterial destruction of labile organic matter; cf. Van Cappellen and Ingall, 1994). This sequence of relative DOA values is also in accord with geochemical and petrographic evidence from the study cores: (1) TS:TC ratios increase northward twice as rapidly in the Stark Shale as in the Hushpuckney Shale (Fig. 12A), suggesting more vigorous sulfate reduction per unit organic carbon in the former formation, possibly due to a greater abundance of labile organic matter for anaerobic decay under strongly anoxic conditions, (2) Fe exhibits a sulfidic affinity in three of four Stark Shale cores but a detrital affinity in all Hushpuckney and Muncie Creek cores (not shown), consistent with stronger sulfidation of Fe in the former formation as inferred from TS-Fe relations (Fig. 9), and (3) I/V ratios increase from the Stark Shale to the Muncie Creek Shale, reflecting greater preservation of more refractory organic matter under less anoxic conditions (Fig. 8A; see discussion of organic matter sources below). If this sequence of relative DOA values for the three study formations is confirmed on a regional scale, it would imply secular variation in the intensity of bottomwater anoxia at maximum transgression from one Midcontinent Pennsylvanian cyclothem to the next (Fig. 13).

**Calibration of DOA Proxies:** Given the existence of regional and stratigraphic trends in redox-sensitive trace-element concentrations, calibration of these trends to a dissolved $O_2$ scale would facilitate delineation of spatio-temporal changes in redox conditions. The most oxygen-depleted conditions in the study area are represented by the proximal Stark Shale (Edmonds core; Fig. 13). The corresponding trace-element proxies for such conditions, which will be assumed equal to 0 ml $O_2$ $l^{-1}$ $H_2O$, are 25.0 for Mo/TC, 12.0 for $U_{exc}$/TC, 0.9 for V/(V+Ni), and 5.0 for V/Cr (Fig. 14A). The least oxygen-depleted conditions in the study area are represented by either the Muncie Creek Shale (Edmonds core) or the distal Stark Shale (Heilman core). This uncertainty exists because the former contains the lowest Mo/TC and $U_{exc}$/TC values (Fig. 11D-E) whereas the latter contains the lowest V/(V+Ni) and V/Cr ratios (Fig. 11F-G); given that V exhibits more variable affinities than Mo or $U_{exc}$ (Table 1), the latter parameters may be more reliable as DOA indicators, implying least oxygen-depleted conditions in the Muncie Creek Shale. The anoxic-dysoxic boundary, i.e., the transition from laminated to weakly bioturbated sediments at ca. 0.2 ml $O_2$ $l^{-1}$ $H_2O$, is roughly coincident with the first occurrence of *Chondrites* burrows in the Muncie Creek Shale at 26 cm, just above the geochemically-analyzed interval at 13-21 cm (Fig. 5). For this reason, values of redox-sensitive trace-element parameters in the Muncie Creek Shale will be taken to represent conditions close to the anoxic-dysoxic boundary, i.e., 6.0 for Mo/TC, 1.5 for $U_{exc}$/TC,

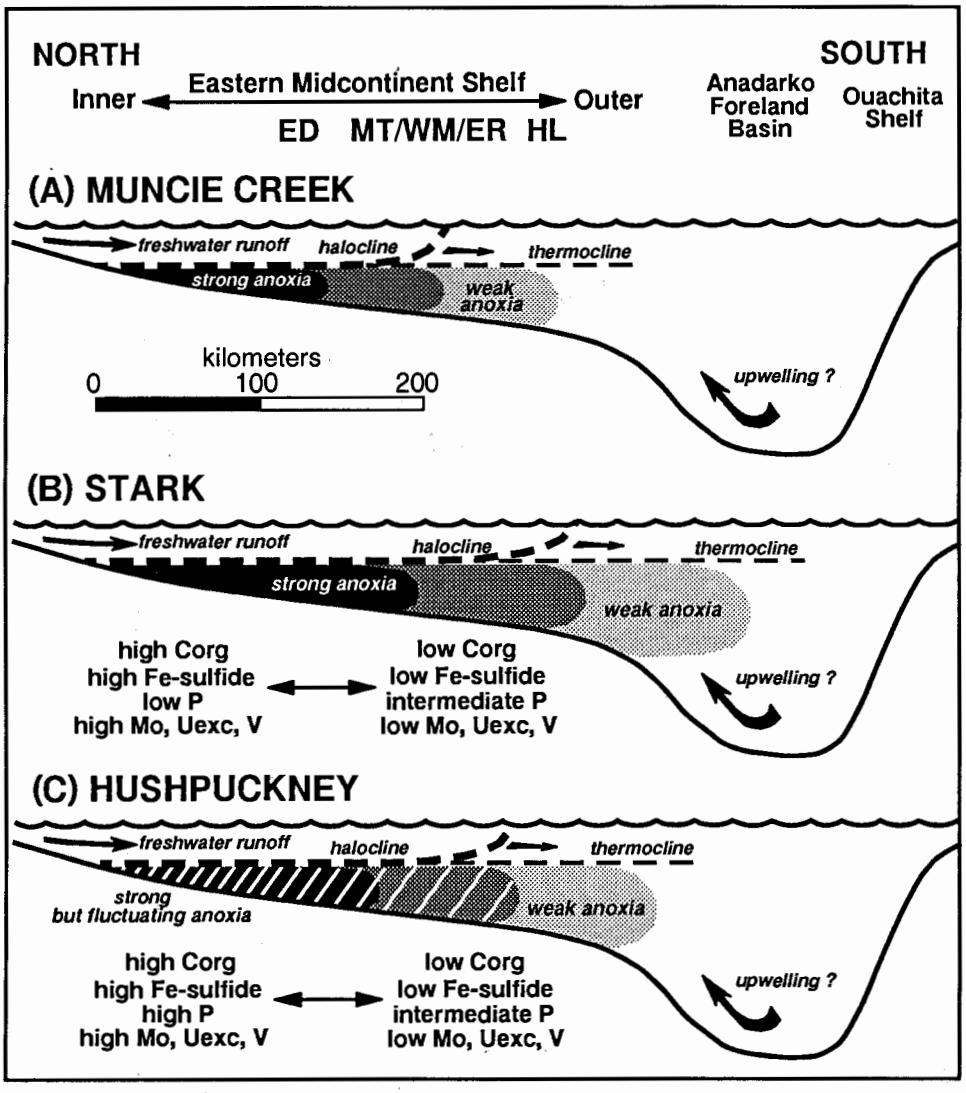


Fig. 13: Interpretative north-south cross-section of environmental conditions on the Eastern Midcontinent Shelf during deposition of the study formations. Regional trends in the concentrations of organic carbon, Fe-sulfide, phosphate, and redox-sensitive trace elements (e.g., Mo, $U_{exc}$, and V) reflect lateral redox gradients, which were due to freshwater runoff from the north, producing a strong proximal halocline a weak distal thermocline (cf. Heckel 1991). Systematic differences in degree-of-anoxia proxies between study formations imply secular variation in redox conditions between cyclothems at maximum transgression: the Muncie Creek environment was the least oxygen depleted (A) and the Stark environment the most strongly anoxic (B). Low but fluctuating $O_2$ levels (diagonally lined fields) promoted phosphate nodule formation in proximal parts of the Hushpuckney environment (C); see text for discussion. Geographic header at top; core abbreviations as in Fig. 8; horizontal scale is approximate.

0.6 for V/(V+Ni), and 1.0 for V/Cr (Fig. 14A). Ultimately, calibration of DOA indices will be facilitated through paleoecological and geochemical analysis of the overlying gray-shale facies (in progress).

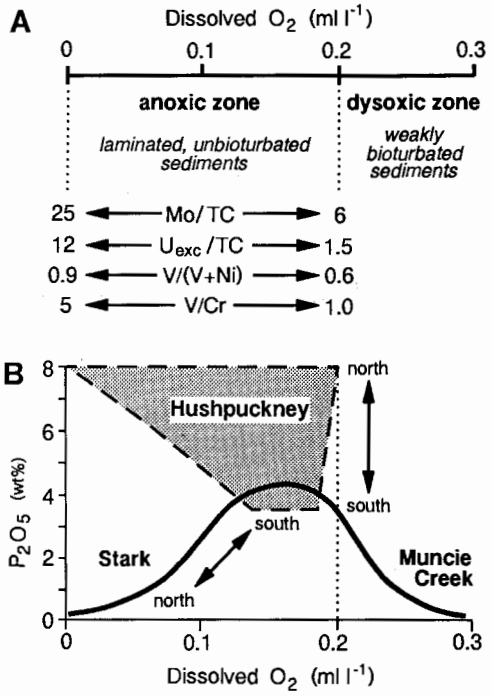


Fig. 14: (A) Calibration of ichnological and geochemical indicators of degree-of-anoxia (DOA). Oxygen-related zones are established on ichnological criteria: the anoxic zone (ca. 0-0.2 ml $O_2$ $l^{-1}$ $H_2O$) is characterized by laminated sediments and the dysoxic zone (ca. 0.2-0.5 ml $O_2$ $l^{-1}$ $H_2O$) by weakly bioturbated sediments. Values of geochemical indicators represent estimates for the lower and upper boundaries of the anoxic zone. (B) Inferred spatio-temporal relations between bottomwater $O_2$ levels and $P_2O_5$ concentrations in the study units. Because most DOA proxies imply decreasing $O_2$ levels northward within the Hushpuckney and Stark shales (Fig. 13), divergent regional trends in $P_2O_5$ concentrations (Fig. 11) suggest differences in P cycling between study formations. At uniformly low $O_2$ levels, remobilized P escapes into the water column (e.g., Stark Shale), whereas at low but fluctuating $O_2$ concentrations (ca. 0-0.2 ml $l^{-1}$), P can be retained through redox cycling of Fe (e.g., Hushpuckney Shale).

**Formation of Authigenic Phosphate:** P fluxes in marine systems are closely linked to organic matter cycling and, hence, bottomwater redox conditions, and the distribution of authigenic phosphate may provide significant information regarding environmental conditions. The geochemical conditions favoring formation of authigenic phosphate have been reviewed recently by Glenn et al. (1994) and Jarvis et al. (1994). Most phosphate is initially precipitated as francolite, a carbonate fluorapatite mineral containing up to 5-6 wt% $CO_2$ and enriched in U, Sr, and Y, which is consistent with elemental associations observed in the study units (Fig. 6). Formation of phosphate nodules depends on a number of factors, the co-occurrence of which is generally transient. Modern phosphates form primarily in offshore areas of high primary productivity, i.e., where the flux of organic matter to the sediments substantially exceeds that of clastic detritus (Burnett, 1980; Burnett et al., 1982). Sediment porewaters must be supersaturated with respect to francolite, which commonly occurs only within a narrow zone in the shallow subsurface where upward diffusing $PO_4^{3-}$ and $CO_3^{2-}$ released from decaying organic matter mix with downward diffusing $Ca^{2+}$, $SO_4^{2-}$ and $F^-$ from the overlying water column. Precipitation occurs mainly at depths of 5-20 cm below the sediment-water interface and is favored by oxygen-depleted, mildly alkaline conditions, such as commonly develop

in the $NO_3^-$ reducing zone (Jarvis et al., 1994). A critical factor in the retention and concentration of sedimentary P may be Fe cycling in association with redox changes within the sediment. Given weakly oxic conditions at or just below the sediment-water interface, iron oxyhydroxides (FeOOH) are precipitated as a solid phase that scavenges dissolved $PO_4^{3-}$ from porewaters. Following burial to depths at which porewaters become anoxic, dissolution of iron oxyhydroxides under reducing conditions liberates both Fe and adsorbed P, which diffuse upward to be reprecipitated in the oxic zone. Redox-related Fe cycling retains P within the shallow subsurface, allowing sufficient time for ionic diffusion and slow growth of phosphate nodules (Burnett et al., 1982). Thus, the most favorable conditions for phosphate precipitation entail bottomwaters that are oxygen-depleted but not fully anoxic (Jarvis et al., 1994), an inference supported by high abundances of phosphate nodules at the upper and lower boundaries of the oxygen minimum zone on modern continental margins at dissolved $O_2$ levels of ca. 0.1-0.2 ml $l^{-1}$, i.e., weakly anoxic conditions (Burnett, 1980).

This model may offer insights on environmental conditions during deposition of Midcontinent Pennsylvanian offshore black shales. In the study units, phosphate nodules formed as authigenic precipitates in the shallow subsurface environment and were not affected by subsequent current winnowing (Fig. 5; Kidder, 1985; Kidder et al., 1996). The present distribution of phosphate nodules probably reflects controls on P retention (i.e., redox conditions) rather than P supply (i.e., organic matter flux), because $P_2O_5$ and TC values exhibit little correlation (not shown). Regional trends in phosphate abundance are diametrically opposed in the Stark and Hushpuckney shales: $P_2O_5$ concentrations are similar at southern locales (ca. 3.5-4.0 wt%) but diverge northward, increasing in the Hushpuckney (to >6 wt%) and decreasing in the Stark (to <1 wt%; Fig. 12C). Because redox-sensitive trace-element parameters suggest more oxygen-depleted conditions northward in both shales, divergent regional phosphate trends imply fundamentally different P cycling processes in these formations. Because retention of P is commonly related to fluctuations in redox conditions near the sediment-water interface, differences in $P_2O_5$ gradients between formations suggest more variable dissolved $O_2$ levels in the Hushpuckney Shale than in the Stark Shale, especially in the northern part of the study area (Fig. 14B). Within each study unit, concentration of phosphate nodules at the upper and lower contacts of organic-rich layers (Fig. 5) implies fluctuations in oxygen levels at a centimeter-scale in the shallow subsurface environment (cf. Hatch and Leventhal, 1992). These observations suggest control of P accumulation in the study units primarily by redox-dependent early diagenetic processes. This conclusion differs from Heckel's (1977, 1991) model for phosphogenesis in Midcontinent Pennsylvanian offshore black shales, which invoked upwelling of nutrient-rich deepwaters and enhanced surfacewater organic productivity.

**Sources of Organic Matter:** Knowledge of the sources of organic matter in a formation can be invaluable in reconstructing environmental controls on its accumulation (e.g., Tyson, 1995). Ideally, the major types of organic components and their distributions within a formation would be determined first and subsequently used in environmental analysis. However, the dominant sources of organic matter in the present study units are not immediately evident, and inferences in this regard can be drawn only cautiously on the basis of relations between petrographic and C-isotopic data. The apparent absence of liptinitic macerals is puzzling in view of earlier studies documenting large quantities of marine algal matter in Midcontinent Pennsylvanian core black shales (Wenger and Baker, 1986; Desborough et al., 1991; Hatch and Leventhal, 1992). In the present study, failure to petrographically detect a liptinitic component may have been due to (1) fine dissemination within the mineral matrix, (2) bacterial reworking to a product resembling vitrinite (cf. Tyson, 1995), or (3) genuine dominance of terrestrial organic matter. Although not conclusive, several factors favor the bacterial reworking hypothesis. First, positive covariation between I/V ratios and bulk organic $\delta^{13}C$ values (not shown, but note positive covariation of both parameters with TOC; Fig. 8A-B) suggests that organic macerals in the study units have different C-isotopic compositions, i.e., ca. -26 to -27 ‰ for inertinite and ca. -28 to -29 ‰ for vitrinite based on mass-balance calculations. The former

Arlington) for editorial handling of the manuscript, to Frank Ettensohn (Univ. of Kentucky) and an anonymous reviewer for thoughtful comments, and to Lisa Trump (Univ. of Cincinnati) for drafting services. Support for this project was provided by the University of Cincinnati Sedimentology Fund and by a GSA Grant-in-Aid (1994) to the senior author.

## References

Algeo, T.J., Phillips, M., Jaminski, J. & Fenwick, M. (1994): High-resolution X-radiography of laminated sediment cores. – J. Sed. Petr. **A64**: 665–668.

Arbenz, J.K. (1989): The Ouachita System. – In: Bally, A.W. & Palmer, A.R. (Eds.): The Geology of North America – An Overview (v. A.). – Geol. Soc. Amer. Boulder, Colorado, 371–396.

Berner, R.A. & Raiswell, R. (1983): Burial of organic carbon and pyrite sulfur in sediments over Phanerozoic time: A new theory. – Geochim. Cosmochim. Acta **47**: 855–862.

Boardman, D.R. & Heckel, P.H. (1989): Glacial-eustatic sea-level curve for early Late Pennsylvanian sequence in north-central Texas and biostratigraphic correlation with curve for midcontinent North America. – Geology **17**: 802–805.

Burnett, W.C. (1980): Apatite-glauconite associations off Peru and Chile: Palaeo-oceanographic implications. – J. Geol. Soc. London **137**: 757–764.

Burnett, W.C., Beers, M.J. & Roe, K.K. (1982): Growth rates of phosphate nodules from the continental margin off Peru. – Science **215**: 1616–1618.

Calvert, S.E. & Pedersen, T.F. (1993): Geochemistry of Recent oxic and anoxic marine sediments: Implications for the geological record. – Mar. Geol. **113**: 67–88.

Canfield, D.E. (1994): Factors influencing organic carbon preservation in marine sediments. – Chem. Geol. **114**: 315–329.

Canfield, D.E., Raiswell, R., Westrich, J.T. Reaves, C.M. & Berner, R.A. (1986): The use of chromium reduction in the analysis of reduced inorganic sulfur in sediments and shales. – Chem. Geol. **54**: 149–155.

Canfield, D.E., Raiswell, R. & Bottrell, S. (1992): The reactivity of sedimentary iron minerals toward sulfide. – Am. J. Sci. **292**: 659–683.

Coveney, R.M., Jr. (1985): Temporal and spatial variations in Pennsylvanian black shale geochemistry. – In: Watney, W.L, Kaesler, R.L. & Newell, K.D. (Eds.): Recent interpretations of Late Paleozoic cyclothems. – 247–266, Kansas Geol. Surv., Lawrence, Kansas.

Coveney, R.M., Jr., Leventhal, J.S., Glasrock, M.D. & Hatch, J.R. (1987): Origins of metals and organic matter in the Mecca Quarry Shale Member and stratigraphically equivalent beds across the Midwest. – Econ. Geol. **82**: 915–933.

Coveney, R.M., Jr. & Shaffer, N.R. (1988): Sulfur-isotope variations in Pennsylvanian shales of the midwestern United States. – Geology **16**: 18–21.

Coveney, R.M., Jr., Watney, W.L. & Maples, C.G. (1991): Contrasting depositional models for Pennsylvanian black shale discerned from molybdenum abundances. – Geology **19**: 147–150.

Crowell, J.C. (1978): Gondwanan glaciation, cyclothems, continental positioning, and climate change. – Am. J. Sci. **278**: 1345–1372.

Crowley, T.J., Hyde, W.T. & Short, D.A. (1989): Seasonal cycle variations on the supercontinent of Pangaea. – Geology **17**: 457–460.

Crowley, T.J. Yip, K.-J., Baum, S.K. & Moore, S.B. (1996): Modelling Carboniferous coal formation. – Paleoclimates **2**: 159–177.

Desborough, G.A., Hatch, J.R. & Leventhal, J.S. (1991): Geochemical and mineralogical comparison of the Upper Pennsylvanian Stark Shale Member of the Dennis Limestone, east-central Kansas, with the Middle Pennsylvanian Mecca Quarry Shale Member of the Carbondale Formation in Illinois and of the Linton Formation in Indiana. – U.S. Geol. Surv. Circ. **1058**: 12–30.

Glenn, C.R., Föllmi, K.B., Riggs, S.R., and 13 others (1994). Phosphorus and phosphorites: Sedimentology and environments of formation. – Eclog. geol. Helv. **87**: 747–788.

Hatch, J.R. & Leventhal, J.S. (1992): Relationship between inferred redox potential of the depositional environment and geochemistry of the Upper Pennsylvanian (Missourian) Stark Shale Member of the Dennis Limestone, Wabaunsee County, Kansas, U.S.A. – Chem. Geol. **99**: 65–82.

Heckel, P.H. (1977): Origin of phosphatic black shale facies in Pennsylvanian cyclothems of midcontinent North America. – Amer. Assoc. Petr. Geol. Bull. **61**: 1045–1068.

– (1984): Factors in Mid-continent Pennsylvanian limestone deposition. – In: Hyne, N.J. (Ed.): Limestones of the Mid-continent. – Tulsa Geol. Soc., Spec. Publ. **2**: 25–50.

– (1986): Sea-level curve for Pennsylvanian eustatic marine transgressive-regressive depositional cycles along midcontinent outcrop belt, North America. – Geology **14**: 330–334.
– (1991): Thin widespread Pennsylvanian black shales of Midcontinent North America: A record of a cyclic succession of widespread pycnoclines in a fluctuating epeiric sea. – In: Tyson, R.V. & Pearson, T.H. (Eds.): Modern and Ancient Continental Shelf Anoxia. – Geol. Soc. London, Spec. Publ. **58**: 259–273.
– (1994): Evaluation of evidence for glacial-eustatic control over marine Pennsylvanian cyclothems in North America and consideration of possible tectonic effects. – In: Dennison, J.M. & Ettensohn, F.R. (Eds.): Tectonic and Eustatic Controls on Sedimentary Cycles. – SEPM (Soc. Sed. Geol.), Tulsa, Oklahoma, Concepts in Sedimentology and Paleontology **4**: 65–87.
Hutton, A.C. (1987): Petrographic classification of oil shales. – Internat. J. Coal Geol **8**: 203–231.
Jaminski, J., Algeo, T.J., Maynard, J.B. & Hower, J.C. (1998): Climatic origin of dm-scale compositional cyclicity in the Cleveland Member of the Ohio Shale (Upper Devonian), Central Appalachian Basin, U.S.A. – In: Schieber, J. et al.: Shales and Mudstones I: 217–242.
Jarvis, I., Burnett, W.C., Nathan, Y., and 9 others (1994): Phosphorite geochemistry: State-of-the-art and environmental concerns. Eclog. geol. Helv. **87**: 643–700.
Jones, B. & Manning, D.A.C. (1994): Comparison of geochemical indices used for the interpretation of palaeoredox conditions in ancient mudstones. – Chem. Geol. **111**: 111–129.
Kidder, D.L. (1985): Petrology and origin of phosphatic nodules from the midcontinent Pennsylvanian epicontinental sea. – J. Sed. Petr. **55**: 809–816.
Kidder, D.L., Hussein, R.A.M., Mapes, R.H. & Eddy-Dilek, C.A. (1996): Regional diagenetic variation in maximum-transgression phosphates from Midcontinent Pennsylvanian shales. – In: Witzke, B.J., Ludvigson, G.A. & Day, J. (Eds.): Paleozoic Sequence Stratigraphy: Views from the North American Craton. – Geol. Soc. Am. Spec. Paper **306**: 351–358.
Lewan, M.D. (1986): Stable carbon isotopes of amorphous kerogens from Phanerozoic sedimentary rocks. – Geochim. Cosmochim. Acta **50**: 1583–1591.
Lewan, M.D. & Maynard, J.B. (1982): Factors controlling the enrichment of vanadium and nickel in the bitumen of organic sedimentary rocks. – Geochim. Cosmochim. Acta **46**: 2547–2560.
Maynard, J.B. (1981): Carbon isotopes as indicators of dispersal patterns in Devonian-Mississippian shales of the Appalachian Basin. – Geology **9**: 262–265.
Parrish, J.T. (1993): Climate of the supercontinent Pangea. – J. Geol. **101**: 215–233.
Pratt, L.M. & Davis, C.L. (1992): Intertwined fates of metals, sulfur, and organic carbon in black shales. – In: Pratt, L.M., Comer, J.B. & Brassell, S.C.: Geochemistry of Organic Matter in Sediments and Sedimentary Rocks. – Soc. Econ. Paleontol. Mineral. Short Course Notes **27**: 1–27.
Rhoads, D.C., Mulslow, S.G., Gutschik, R., Baldwin, C.T. & Stolz, J.F. (1991): The dysaerobic zone revisited: A magnetic facies? – In: Tyson, R.V. & Pearson, T.H. (Eds.): Modern and Ancient Continental Shelf Anoxia. – Geol. Soc. London Spec. Publ. **58**: 187–199.
Savrda, C.E. & Bottjer, D.J. (1991): Oxygen-related biofacies in marine strata: An overview and update. – In: Tyson, R.V. & Pearson, T.H. (Eds.): Modern and Ancient Continental Shelf Anoxia. – Geol. Soc. London Spec. Publ. **58**: 201–219.
Savrda, C.E., Bottjer, D.J. & Seilacher, A. (1991): Redox-related benthic events. – In: Einsele, G., Ricken, W. & Seilacher, A. (Eds.): Cycles and Events in Stratigraphy. – 524–541, Springer, Berlin.
Schultz, R.B. & Coveney, R.M., Jr. (1992): Time-dependent changes for Midcontinent Pennsylvanian black shales. – Chem. Geol. **99**: 83–100.
Schutter, S.R. & Heckel, P.H. (1985): Missourian (Early Late Pennsylvanian) climate in Midcontinent North America. – Internat. J. Coal Geol. **5**: 111–140.
Scotese, C.R. (1994): Carboniferous paleocontinental reconstructions. – U.S. Geol. Surv.-Bull. **2110**: 3–6.
Tyson, R.V. (1995): Sedimentary Organic Matter. – 615pp., Chapman & Hall, London.
Van Cappellen, P. & Ingall, E.D. (1994): Benthic phosphorus regeneration, net primary production, and ocean anoxia: A model of the coupled marine biogeochemical cycles of carbon and phosphorus. – Paleoceanography **9**: 677–692.
Veevers, J.J. & Powell, C.M. (1987): Late Paleozoic glacial episodes in Gondwanaland reflected in transgressive-regressive depositional sequences in Euramerica. – Geol. Soc. Am. Bull **98**: 475–487.
Watney, W.L., French, J.A. & Franseen, E.K. (1989): Sequence stratigraphic interpretations and modeling of cyclothems in the Upper Pennsylvanian (Missourian) Lansing, and Kansas City groups in eastern Kansas. – Kansas Geol. Soc., Lawrence, Kansas, 41st Annual Fieldtrip Guidebook, 211 pp.
Wenger, L.M. & Baker, D.R. (1986): Variations in organic geochemistry of anoxic-oxic black shalecarbonate sequences in the Pennsylvanian of the Midcontinent, U.S.A. – Org. Geochem. **10**: 85–92.
Wignall, P.B. (1994): Black Shales. – 127 pp., Clarendon Press, Oxford.

Wignall, P.B. & Myers, K.J. (1988): Interpreting benthic oxygen levels in mudrocks: A new approach. – Geology, **16**: 452–455.

Addresses of the authors:

David L. Hoffman, Thomas J. Algeo, J. Barry Maynard and Jacek Jaminski, H. N. Fisk Laboratory of Sedimentology, Department of Geology, University of Cincinnati, Cincinnati, Ohio 45211-0013, U.S.A.
Michael M. Joachimski, Institut für Geologie, Universität Erlangen-Nürnberg, D-91054 Erlangen.
James C. Hower, Center for Applied Energy Research, 3572 Iron Works Pike, Lexington, Kentucky 40511-8433, U.S.A., and Department of Geological Sciences, University of Kentucky, Lexington, Kentucky 40506-0059, U.S.A.